On the Calibration of Direct-Current Current Transformers (DCCT)

(Article begins on next page)

26 November 2024

On the calibration of direct-current current transformers

Luca Callegaro, Cristina Cassiago, and Enrico Gasparotto [*][†]

Abstract

Modern commercial direct-current current transformers (DCCT) can measure currents up to the kA range with accuracies better than 1×10^{-5}. We discuss here a DCCT calibration method and its implementation with commercial instruments typically employed in low resistance calibration laboratories. The primary current ranges up to $2\,\mathrm{kA}$; in the current range below $100\,\mathrm{A}$ the calibration uncertainty is better than 3×10^{-7}. An example of calibration of a high-performance DCCT specified for primary currents measurement up to $900\,\mathrm{A}$ is discussed in detail.

1. INTRODUCTION

Commercial direct-current current transformers (DCCT) are the most accurate dc high-current sensors available [1], with specified relative accuracies in the 10^{-5} range and integral linearities better than 1×10^{-6}. The verification of such high performances, and the calibration of the DCCT ratio, ask for metrological facilities capable of handling the high currents required, of high accuracy and with automated operability [2–5].

Ultimate current ratio accuracy is achieved in cryogenic current comparators (CCC) [6]. In a CCC, the ratio accuracy is given by constraining the magnetic flux path (generated by the current being compared) within superconducting shields; an extreme sensitivity is given by a superconducting quantum interference device (SQUID) flux sensor. Even though CCCs capable of handling currents up to $100\,\mathrm{A}$ have been realized [7], these devices are research instruments not available in calibration laboratories.

Ferromagnetic-core, room-temperature current comparators (CC) are current ratio devices which can achieve ratio errors (deviations from reading) better than 1×10^{-7} [8], and can be self-calibrated through step-up procedures [9, 10] with similar levels of uncertainty. Thus, a CC can act as the current ratio standard in a DCCT calibration setup. Although complex and expensive instruments, high-current CC are a common presence in electrical calibration laboratories, since they are embedded within commercial resistance ratio bridges employed for the measurement of low-valued resistance standards. Such instruments include also current sources, detectors, and firmware for automated operation.

Here we present a simple circuit that allows the calibration of the ratio of a DCCT by using commercial components, originally designed for the calibration of low-valued resistors. The accuracy reached is dependent on the primary current and can be lower than 3×10^{-7} for currents below $100\,\mathrm{A}$. An example of calibration of a DCCT having a $1500 : 1$ nominal ratio for currents up to $900\,\mathrm{A}$ is reported.

The implementation has been employed for the participation to the EURAMET.EM-S35 High DC current ratio supplementary comparison [11], in which INRIM acts as co-pilot laboratory.

2. THE METHOD

Fig. 1 shows the schematics of the calibration setup.

The instruments employed are, in addition to the DCCT under calibration, an automated current range extender EXT and a current comparator ratio bridge CC.

All these instruments are based on the same principle: a high-permeability ferromagnetic core is wound by $m + 1$ windings, each of N_k turns, through which currents I_k flow. The magnetic equation of such circuit is $\sum_k N_k I_k = \mathcal{R}\Phi$, where Φ is the flux in the magnetic core and $\mathcal{R}$ its magnetic reluctance. Φ is measured by a dc flux detector (based on the fluxgate modulation technique [1, 12, 13]) which output acts as error signal for the feedback control of a current generator I_0 connected to winding N_0. The goal of the feedback control is to achieve $\Phi = 0$, which results in the ampere-turns balance equation $\sum_{k=0}^{m} N_k I_k = 0$.

In both DCCT and EXT, only two windings ($m = 1$) are active in a given operating condition. The controlled current generator output I_0 constitutes the device output current; the primary current I_1 is

---

[*]Luca Callegaro, Cristina Cassiago and Enrico Gasparotto are with the Electromagnetism Division of the Istituto Nazionale di Ricerca Metrologica (INRIM), Strada delle Cacce 91, 10135 Torino, Italy, e-mail: l.callegaro@inrim.it

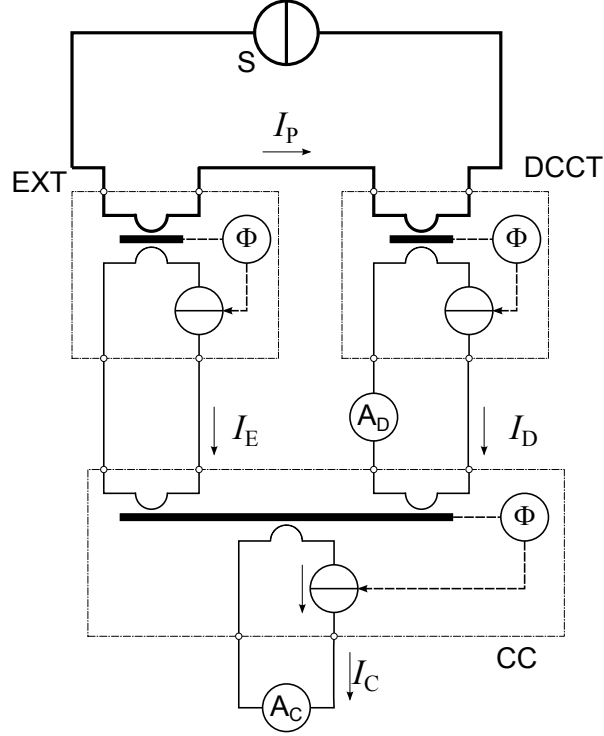[†]Manuscript received March 4, 2014.

Figure 1: Principle schematics of the DCCT calibration setup. S is the high-current source, EXT is an automated current range extender, CC a dc current comparator. Meter A_D monitors the DCCT output I_E; meter A_C give the reading of I_C employed in the measurement model Eq. (2).

thus scaled down with the turns ratio $t = \frac{N_1}{N_0}$ as $I_0 = tI_1$. In CC, more windings ($m \geq 2$) are active; currents can be compared, weighted by their respective winding turns; a measurement of the controlled current generator output allows the determination of the primary current unbalances.

In Fig. 1, the input windings of both DCCT and EXT, are connected in series and fed by the primary current I_P generated by a high-current dc source S. DCCT and EXT output currents are $I_D = G_D I_P$, and $I_E = G_E I_P$ respectively; G_D is the DCCT current gain (that is, the measurand), and G_E is the EXT current gain.

I_D and I_E are connected to two input windings of CC, each having N_D and N_E turns. I_D is also measured by a high-accuracy ammeter A_D.

The CC compensation current I_C, linked to CC winding of turns N_C, is measured by ammeter A_C; when operating properly, the CC balance equation is

$$N_E I_E + N_D I_D + N_C I_C = 0. \tag{1}$$

In Eq. (1), the sign of turn numbers N_x can be either positive or negative and is set by the winding direction on the core.

When all automated controls operate properly, each core flux is drawn to zero, and the balance equation is of the whole circuit becomes

$$G_D = \frac{I_C}{I_P}\frac{N_C}{N_D} - G_E \frac{N_E}{N_D}. \tag{2}$$

A relative gain error δG_D respect to nominal gain $G_D^{(n)}$ can also be computed,

$$\delta G_D = \frac{G_D - G_D^{(n)}}{G_D^{(n)}}. \tag{3}$$

All instruments based on the fluxgate technique suffer from a certain degree of dc offset, caused by the magnetization hysteresis and relaxation of the ferromagnetic core. This offset, in the order of 1×10^{-5} A per unit input turn [12], is dependent on temperature, measurement history and drifts with time. To compensate for these offset, the reading I_{C} in Eq. (2) is substituted with $\Delta I_{\mathrm{C}} = I_{\mathrm{C}} - I_{\mathrm{C}0}$, where $I_{\mathrm{C}0}$ is the reading taken with null primary current $I_{\mathrm{P}} = 0$.

3. IMPLEMENTATION

A test implementation of the schematic of Fig. 1 has been set up with the following instrumentation:

- DCCT under calibration. Results reported in Sec. 4. refer to a LEM mod. ITN 900-S ULTRASTAB high-performance current transducer [14]. Primary current $|I_{\mathrm{P}}| \leq 900$ A, nominal ratio $G_{\mathrm{D}} = 1/1500$, accuracy better than 2×10^{-5} (including offset), linearity better than 1×10^{-6}, maximum resistance of the burden $2.5\,\Omega$. Fig. 2 shows the DCCT mounted on the primary busbar.
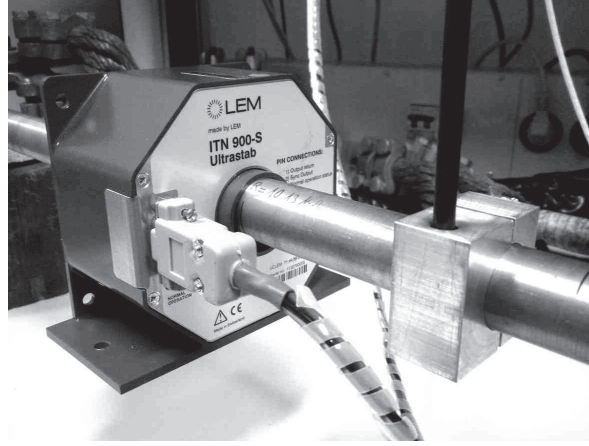

Figure 2: The DCCT under calibration mounted on the primary current busbar. Placed on the busbar is also an aluminum block (foreground) that includes a thermometer head for temperature monitoring.

- CC: Guildline mod. 9920 direct current comparator. This instrument is particularly flexible since it provides several fixed windings having a decadic (1 to 1000) number of turns, one winding with an adjustable number of turns through decade rotary switches, and allows a full reconfiguration of the connections between the windings and the internal electronics. The setting for the DCCT being calibrated is $N_{\mathrm{D}} = -100$ (fixed winding), $N_{\mathrm{E}} = 150$ (decade winding). $N_{\mathrm{C}} = 1$, in order to achieve the largest sensitivity in the measurement of I_{C}.

- EXT: Two different extenders have been employed, depending on I_{P}:

    - Measurement International mod. MI 6011B range extender. $|I_{\mathrm{P}}| \leq 100$ A, nominal ratio $1/1000$, relative accuracy $< 1 \times 10^{-7}$.

    - Measurement International mod. MI 6012M range extender, $|I_{\mathrm{P}}| \leq 2$ kA, nominal ratio $1/1000$, relative accuracy $< 2 \times 10^{-6}$.

    The performances of these instruments can be validated in the original low-resistance measurement setups for which they are designed [15].

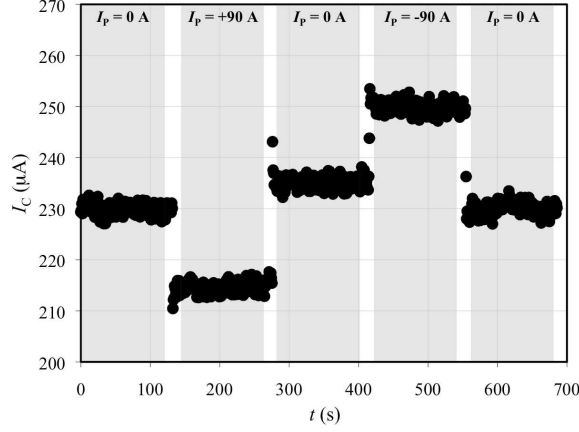- S: two different sources have been employed, depending on the primary current I_{P}:

Figure 3: Time recording of the compensation current I_C for different primary currents I_P.

- Measurement International MI 6100A linear dc power supply, current output $0\,\text{A}$ to $+100\,\text{A}$. Current reversal is achieved with a switch internal to MI 6011B.

- Agilent mod. 6680A, current output up to $875\,\text{A}$. Two items are connected in parallel, and a Measurement International mod. 6025 pneumatic switch allows the current reversal.

- A_D: an Agilent mod. 3458A multimeter, in dc voltage mode, measures the voltage drop on a Tinsley mod. 1659 $1\,\Omega$ standard resistor.

- A_C: a second 3458A multimeter in dc current mode, $100\,\text{mA}$ range.

The DCCT and busbar temperatures are monitored with two PT100 platinum thermoresistance elements read by a Fluke mod. 1529 CHUB E-4 thermometer. Fig. 2 shows the location of the busbar thermometer head.

4. RESULTS

The gain error δG_D defined in Sec. 2. asks for the determination of $\Delta I_C = I_C - I_{C0}$, where the two readings I_C and I_{C0} correspond to the nominal current $I_P^{(n)}$ of interest, and to a zero current $I_P = 0$. The measurement system is therefore run continuously, and I_P is cycled periodically between values 0, $+I_P^{(n)}$, 0, $-I_P^{(n)}$ and so on; the reading I_C is continuously recorded. Fig. 3 shows a time series of I_C readings corresponding to an I_P cycle. For each value of I_P, after transients have died out, a time average $\overline{I_C}(I_P)$ is computed (see gray bands in Fig. 3).

The quantity ΔI_C to be employed in Eq. (2) is computed as $\Delta I_C(I_P^{(n)}) = \overline{I_C}(I_P^{(n)}) - (\overline{I_C'}(0) + \overline{I_C''}(0))/2$, where $\overline{I_C'}(0)$ and $\overline{I_C''}(0)$ are the zero readings respectively preceding and succeeding $\overline{I_C}(I_P^{(n)})$ in the time series.

From each $\Delta I_C(I_P^{(n)})$, the absolute $\Delta G_C(I_P^{(n)})$ and relative $\delta G_C(I_P^{(n)})$ errors are computed. Fig. 4 graphically shows the values δG_D corresponding to each $I_P^{(n)}$ measurement cycle. Tab. 1 reports the estimates for G_D and δG_D of the DCCT under measurement, together with the corresponding $95\,\%$ expanded uncertainties, for several primary current $I_P^{(n)}$ values.

As an example, the uncertainty budget for the calibration of G_D at $I_P = +90\,\text{A}$ is given in Tab. 2, where it can be appreciated that the principal contributions to measurement uncertainty are the measurement repeatability of I_C and the EXT ratio N_E/N_D.

5. CONCLUSIONS

The setup proposed allows the calibration of the ratio of a DCCT with accuracies in the 10^{-6} range or better. The proposed implementation, suitable for primary currents up to $2\,\text{kA}$, is based on commercial
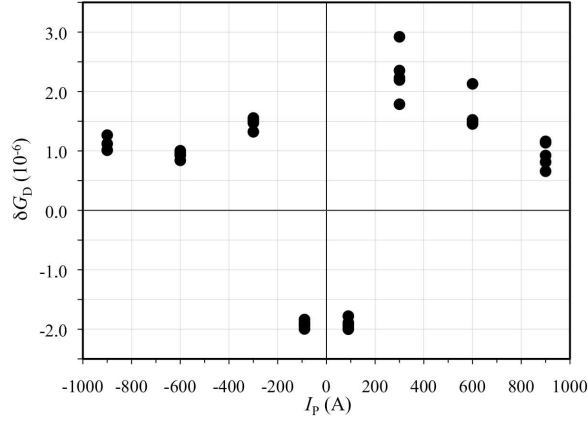
Figure 4: The relative gain error δG_D of the DCCT under calibration, for different nominal primary current values $I_P^{(n)}$. Each dot corresponds to half of the measurement cycle shown in Fig. 3. For each $I_P^{(n)}$, five measurement results are reported. The average value and its uncertainty are given in Tab. 1.

Table 1: DCCT gain G_D for different primary currents I_P. The relative deviation δG_D from nominal ratio is also reported.

$I_P^{(n)}$ A	Supply	EXT	G_D $\times 10^{-4}$	δG_D $\times 10^{-6}$	$U(\delta G_D)$ $\times 10^{-6}$
+90	6100A	6011B	6.666 653 9(16)	−1.92	0.24
−90	6100A	6011B	6.666 653 9(16)	−1.92	0.23
+300	6680A	6012M	6.666 682(16)	+2.3	2.3
−300	6680A	6012M	6.666 676(15)	+1.5	2.3
+600	6680A	6012M	6.666 677(15)	+1.6	2.3
−600	6680A	6012M	6.666 676(15)	+0.9	2.3
+900	6680A	6012M	6.666 672(15)	+0.9	2.3
−900	6680A	6012M	6.666 673(15)	+1.1	2.3

instruments typically employed for low-resistance calibrations, and therefore often available in calibration laboratories. The implementation has been employed for the participation to the EURAMET.EM-S35 comparison. The result of the comparison, when available, will therefore constitute a validation of the implementation.

ACKNOWLEDGMENTS

REFERENCES

[1] P. Ripka, "Electric current sensors: a review," *Meas. Sci. Technol.*, vol. 21, p. 112001, 2010, 23 pp.

[2] M. Zhu and K. Xu, "A calibrating device for large direct current instruments up to 320 kiloampere-turns," *Instrumentation and Measurement, IEEE Transactions on*, vol. 47, no. 3, pp. 711–714, Jun 1998.

[3] G. Fernqvist, J. Pett, and J. Pickering, "A reference standard system based on dc current," in *Precision Electromagnetic Measurements, 2002. Conference Digest 2002 Conference on*, June 2002, pp. 164–165.

[4] G. Fernqvist, B. Halvarsson, J. Pett, and J. Pickering, "A novel current calibration system up to 20 kA," *Instrumentation and Measurement, IEEE Transactions on*, vol. 52, no. 2, pp. 445–448, April 2003.

Table 2: Uncertainty budget for G_D, at $I_P^{(n)} = +90$ A.

Quantity	X	$u(X)$	contrib. to $u(G_D)$	type
ΔI_C	$-17.2\,\mu A$	$0.36\,\mu A$	2.7×10^{-11}	A
I_P	$90\,A$	$90\,mA$	1.3×10^{-12}	B
N_C/N_D	$-6.666\,666\,7 \times 10^{-3}$	6.7×10^{-10}	$< 1 \times 10^{-13}$	B
N_E/N_D	$-6.666\,666\,7 \times 10^{-1}$	6.7×10^{-8}	6.7×10^{-11}	B
G_E	$+1.000\,000\,0 \times 10^{-3}$	5.8×10^{-11}	3.8×10^{-11}	B
G_D	$+6.666\,653\,9 \times 10^{-4}$	8.1×10^{-11}		
δG_D	-1.92×10^{-6}	1.2×10^{-7}		
$U_{R95}(\delta G_D)$		2.4×10^{-7}		

[5] G. Hudson, B. Jeckelmann, and J.-D. Baumgartner, "Comparison of cern and metas high current standards up to 10ka," in *Precision Electromagnetic Measurements Digest, 2008. CPEM 2008. Conference on*, June 2008, pp. 548–549.

[6] J. M. Williams, "Cryogenic current comparators and their application to electrical metrology," *IET Science, Measurement & Technology*, vol. 5, no. 6, pp. 211–224, 2011.

[7] J. M. Williams and P. Kleinschmidt, "A cryogenic current comparator bridge for resistance measurements at currents of up to 100 A," *IEEE Trans. Instr. Meas.*, vol. 48, no. 2, pp. 375–378, 1999.

[8] W. J. M. Moore and P. N. Miljanic, *The current comparator*, ser. IEE electrical measurement series. London, UK: Peter Peregrinus Ltd, 1988, vol. 4, iSBN 0863411126.

[9] H. Shao, F. Lin, X. Hua, B. Liang, K. Qu, and Y. Pan, "DC high current ratio standard based on series-parallel calibration method," in *Precision Electromagnetic Measurements (CPEM) Conf.*, Jun. 2010, pp. 535 –536.

[10] H.-G. Zhao, X.-Z. Zhang, Y. Liu, L.-Y. Zheng, and B.-X. Zou, "Calibration of DC current up to 600 A," in *Precision Electromagnetic Measurements (CPEM) Conf. on*, Jun. 2010, pp. 603 –604.

[11] C. Cassiago and A. Mortara, "Comparison of high-current ratio standard," EURAMET, Technical Protocol 1217, Feb 2012, available online at www.euramet.org.

[12] M. P. MacMartin and N. L. Kusters, "A direct-current-comparator ratio bridge for four-terminal resistance measurements," *IEEE Trans. Instr. Meas.*, vol. 15, no. 4, pp. 212 –220, Dec 1966.

[13] P. Odier, "DCCT technology review," in *Proc. of Workshop on DC current transformers and beam-lifetime evaluations*, A. Peters, H. Schmickler, and K. Wittenburg, Eds. Lyon, France: CARE-HHH-ABI Networking, 1-2 Dec 2004, pp. 3–5.

[14] W. Teppan and D. Azzoni, "Closed-loop fluxgate current sensor," European Patent EP2 251 704A1, 2010.

[15] M. Kraft, "Measurement techniques for evaluating current range extenders from 1 ampere to 3000 ampere," *NCSLI Measure J. Meas. Sci.*, vol. 7, no. 3, pp. 32–36, Sep 2012.